

Optogenetic Engineering: Light-Directed Cell Motility**

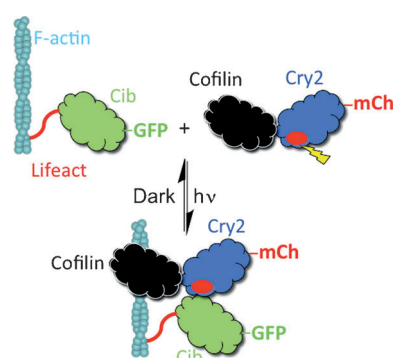
Robert M. Hughes and David S. Lawrence*

Abstract: Genetically encoded, light-activatable proteins provide the means to probe biochemical pathways at specific subcellular locations with exquisite temporal control. However, engineering these systems in order to provide a dramatic jump in localized activity, while retaining a low dark-state background remains a significant challenge. When placed within the framework of a genetically encodable, light-activatable heterodimerizer system, the actin-remodelling protein cofilin induces dramatic changes in the F-actin network and consequent cell motility upon illumination. We demonstrate that the use of a partially impaired mutant of cofilin is critical for maintaining low background activity in the dark. We also show that light-directed recruitment of the reduced activity cofilin mutants to the cytoskeleton is sufficient to induce F-actin remodeling, formation of filopodia, and directed cell motility.

Chemical and optogenetic methods for clustering proteins at subcellular locations have flourished in recent years.^[1] However, in spite of the promise that optogenetic tools hold for biology and medicine,^[2] their ready application is constrained by “protein engineering strategies that unfortunately remain in [the] development stage”.^[3] Engineering challenges include the high levels of dark (background) activity that inadvertently up- or downregulate genes and biochemical pathways of interest. Several strategies have been described to address this and related issues, including protein sequestration and subsequent release,^[4] the use of split protein constructs that are only active upon reconstitution,^[5] and the application of nonsense suppression technology to introduce nonstandard amino acids.^[6] Each of these strategies offers elegant solutions to the construction of light-activated proteins. However, these methods require a level of biochemical and cellular engineering that is beyond the expertise typically available in most biology labs.

We describe herein an optogenetic engineering approach that draws its inspiration from the Michaelis–Menten equation ($v_0 = k_{\text{cat}}[E][S]/(K_m + [S])$). In particular, the latter asserts the dependence of catalytic rate on both the intrinsic k_{cat} of

the enzyme as well as its concentration.^[7] An enzyme with significantly impaired activity could have the reaction velocity restored by concentrating the catalyst in a spatially well-defined fashion. If the latter were achieved in a light-mediated manner then activity in the dark should be minimal, whereas activity upon illumination could equal that of wild-type protein (Scheme 1). Indeed, this strategy should prove applicable to any protein, whether or not it is a catalyst, as long as its activity can be controlled in a concentration-dependent fashion.



Scheme 1. General strategy for the design of a genetically encoded light-activatable protein. A weakly active cofilin mutant (black) is appended to the light-responsive Cry2 (blue). In the absence of light, the cofilin construct has no discernable effect on the cytoskeleton. Upon illumination at 488 nm, Cry2 associates with F-actin-bound Cib (green), furnishing a high, effective cofilin concentration, thereby promoting F-actin severing, cytoskeleton remodelling, lamellipodia formation, and directed cell motility.

Building upon previous work that examined the structure–function relationships of cofilin, we introduced D94A, S120A, K96Q mutations, which are known to impair the F-actin-binding, severing, and depolymerizing activity of cofilin (see Figure S1 a in the Supporting Information).^[8] In addition, we introduced an Ala-for-Ser mutation at the S3 position to ensure that cofilin cannot be intracellularly “turned off” through phosphorylation.^[9] In short, we anticipated that a constitutively active cofilin (S3A) with poor F-actin affinity and reduced F-actin severing (D94A, S120A, K96Q) should display a higher concentration threshold for efficient F-actin severing and depolymerization relative to wild-type cofilin (Table 1; Figures S1 b,c and S2).

The activity of the isolated S3A/D94A, S3A/S120A, and S3A/K96Q proteins was assessed using a pyrene-labelled actin assay.^[10] The S3A/S120A double mutant displays an order of magnitude minimal to maximal activity range (0.2–5 μM , Table 1). This dynamic range recapitulates the minimal activity displayed by disabled S3E cofilin and the robust

[*] Prof. Dr. R. M. Hughes, Prof. Dr. D. S. Lawrence
Department of Chemistry, Division of Chemical Biology and Medicinal Chemistry, and Department of Pharmacology
University of North Carolina
Chapel Hill, NC 27599 (USA)
E-mail: lawrencd@email.unc.edu

[**] We thank the NIH for financial support (1R01CA159189). We are grateful to Prof. James Bamberg (Colorado State) for helpful discussions regarding the manuscript. MTLn3 cells were a gift from Prof. James Bear (UNC). LifeAct-mTurq2 was a gift from Prof. Theodor W. J. Gadella (University of Amsterdam). pNic28-BSA4 was a gift from the Toronto Structural Genomics Consortium.



Supporting information for this article is available on the WWW under <http://dx.doi.org/10.1002/anie.201404198>.

Table 1: Summary of actin–pyrene assays of cofilin single and double mutants at indicated cofilin concentrations.

[Cofilin] [μM]	WT	S3E	S3A	S3A S120A	S3A D94A	S3AK96Q
0.2	++	–	++	–	–	–
0.5	+++	–	+++	+	–	–
1	+++	–	+++	++	–	–
5	n.d.	+	n.d.	+++	+	++
10	n.d.	++	n.d.	+++	+	+++
20	n.d.	++	n.d.	+++	+	+++
40	n.d.	++	n.d.	+++	+	+++

“–” = no severing; “+” = weak severing; “++” = moderate severing; “+++” = strong severing; n.d. = not determined. See Figures S1 and S2 for real-time plots.

activity exhibited by constitutively active S3A cofilin. Although the other double mutants, S3A/D94A and S3A/K96Q, display concentration-dependent F-actin remodelling, neither are as active as S3A/S120A construct. We confirmed that the reduced activity of these cofilin mutants is due, at least in part, to reduced F-actin-binding affinity (Figure S1 c).

We subsequently incorporated fully active S3A cofilin and its activity-compromised counterparts into a light-activatable dimerizer system, cryptochrome 2–Cib (Cry2–Cib; Scheme 1).^[1b] This light-responsive construct enjoys the advantage of rapid dimerization activated by blue light (488 nm). A fluorescent Cib construct that is anchored to F-actin was prepared: LifeAct–Cib–GFP. The LifeAct component is efficiently incorporated into the F-actin network and has little effect on actin dynamics.^[11] The other half of the light-induced dimerizer system is comprised of a fully active truncated form of Cry2 fused to mCherry (Cry2–mCh) (Scheme 1), which is homogeneously distributed throughout the cytoplasm in the dark. However, upon illumination, Cry2–mCh rapidly translocates to the F-actin network in REF52, Cos7, and MTLn3 cells (Figure 1, Movie S1 in the Supporting Information). Upon cessation of illumination, Cry2–mCh fully dissociates from F-actin within six minutes (Figure S3 a). Consequently, the construct is both light-activatable and dark-reversible.

With the light-sensitive dimerizer in hand, fully functional and reduced-activity cofilin constructs were appended to the N and C termini of the Cry2–mCh scaffold (Scheme 1; Figure S3 b). We initially characterized these Cof–Cry2 fusions using whole-cell illumination to visualize cofilin recruitment to F-actin in MTLn3 cells. These experiments revealed that all the cofilin constructs exhibit a rapid light-induced translocation to the cytoskeleton, but with varied F-actin residence times: CofS3A–Cry2–mCh < CofS3A.S120A–Cry2–mCh < CofS3E–Cry2–mCh (Figure S3 c,d). The intracellular F-actin residence time inversely correlates with the activity of the cofilin mutant, implying that the actin-binding and severing/depolymerizing activity of the cofilin constructs play a role in the rate of dissociation of the dimer pair. The C-terminal cofilin mutants exhibit a similar trend, with the F-actin residence time inversely mirroring the activity of the cofilin mutant.

Co-transfection of MTLn3 cells with the Cof–Cry2–mCh constructs and LifeAct–mTurq2 (to visualize the F-actin

network) revealed that the wild type and the constitutively active S3A mutant bind to the cortical F-actin network and other F-actin-rich structures in the dark (Figure 2 a,b). By contrast, the partially impaired S3A.S120A construct and the significantly impaired S3E construct do not associate with F-actin in the absence of illumination (Figure 2 c and Figure S4). This result is consistent with the known inability of the S3E mutant to associate with the actin network.^[12] These results demonstrate that, in the dark, fully active constructs impact cytoskeletal dynamics, whereas functionally impaired cofilin mutants do not.

We subsequently carried out global illumination experiments of MTLn3 cells to assess the consequences of cofilin recruitment on the F-actin network. MTLn3 cells were simultaneously imaged and stimulated by illumination at 488 nm once every minute over a ten minute time course using a confocal microscope at a scan rate of 4 $\mu\text{sec}/\text{pixel}$. Cells containing the CofS3A.S120A–Cry2–mCh construct display a 10% expansion in cell area upon illumination (Figure S5), which is consistent with earlier studies showing that upregulation of cofilin activity (by epidermal growth factor) induces cell spreading.^[13] By contrast, cells with the control Cry2–mCh construct exhibit a slight global retraction. Additional global illumination experiments were conducted with a wide-field microscope in order to capture all the changes at the cell periphery. This experiment revealed the formation of numerous filopodia upon cofilin recruitment (Figure 3), a response similar to that produced by treating MTLn3 cells with EGF,^[14] which is known to upregulate cofilin activity.^[10a]

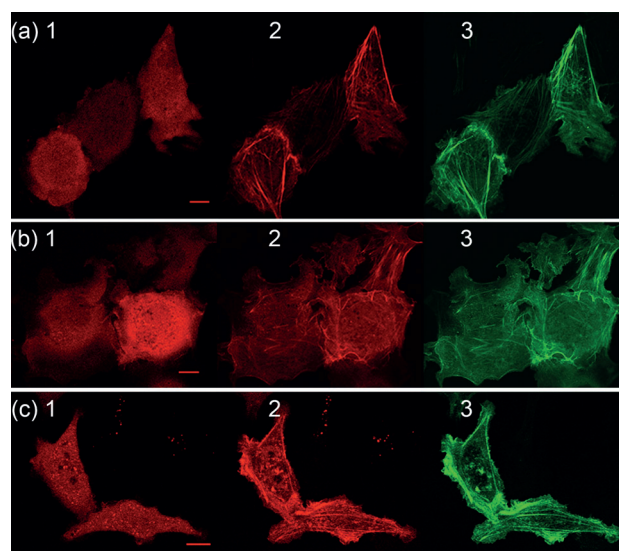


Figure 1. Visualization of light-mediated (488 nm laser, 4 $\mu\text{s}/\text{pixel}$ scan rate, 5% laser power) Cry2–mCh recruitment to LifeAct–Cib–GFP/F-actin in a) REF52, b) COS-7, and c) MTLn3 cells. 1) Pre-illumination imaging of Cry2–mCh demonstrates that the construct is distributed throughout the cytoplasm, 2) post-illumination (10 s) imaging of Cry2–mCh shows accumulation at F-actin as assessed by 3) imaging of LifeAct–Cib–GFP. Pearson’s coefficient of (2) and (3) is a) 0.93 ± 0.02 , b) 0.96 ± 0.03 , and c) 0.93 ± 0.03 ; $n = 8$. Scale bar = 10 μm .

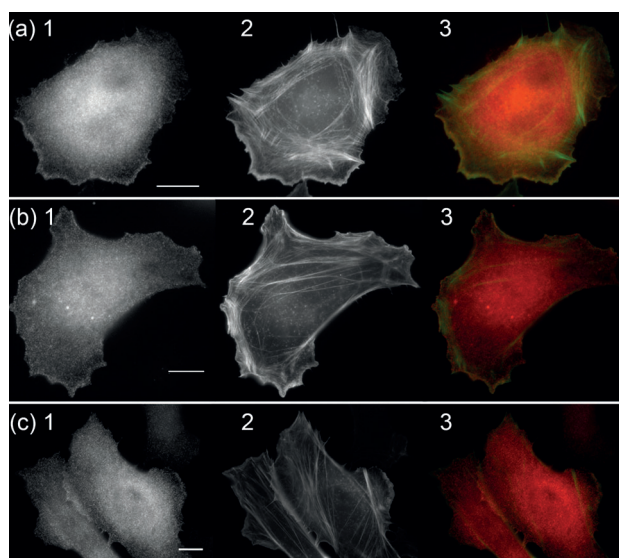


Figure 2. Interaction of Cof-Cry2-mCh constructs with F-actin in the dark (“background activity”) in MTLn3 cells. a) Cof(WT)-Cry2-mCh, b) CofS3A-Cry2-mCh, and c) CofS3A.S120A-Cry2-mCh. See Figure S4 for CofS3E-Cry2-mCh. 1) Cof-Cry2-mCh distribution, 2) F-actin distribution imaged through LifeAct-mTurq2, and 3) overlay highlighting colocalization (green) between the cofilin constructs and F-actin. (a) and (b) display significant co-localization (green), whereas (c) and the S3E construct (Figure S4) do not. Scale bar = 5 μm .

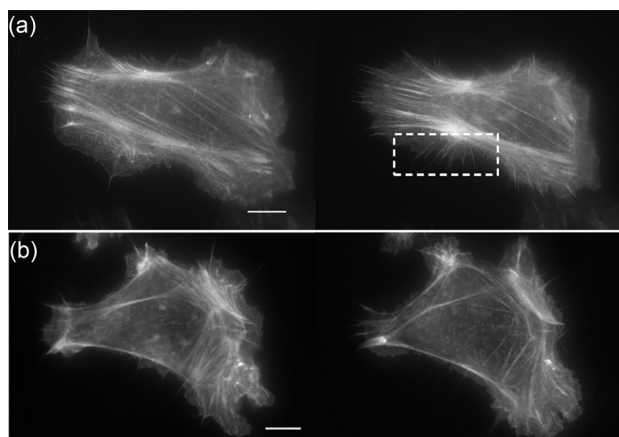


Figure 3. Cofilin-induced filopodia in MTLn3 cells. a) F-actin network of an MTLn3 cell transfected with CofS3A.S120A-Cry2-mCh/LifeAct-Cib-GFP prior to (left) and 10 min after (right) illumination. b) F-actin network of a Cry2-mCh/LifeAct-Cib-GFP transfected MTLn3 cell prior to (left) and 10 min after (right) illumination. Numerous filopodia were formed in the cofilin-transfected cells following light stimulation [highlighted in (a)]. Eight cells total were examined with the above light exposure protocol and filopodia counted at prior to and following illumination. Cofilin-expressing cells have a mean four-fold increase in filopodia (3.6 ± 0.8), while control cells exhibit a negligible change in filopodial structures (1.3 ± 0.2) $n = 10$; $**p = 0.001$, one way ANOVA. See Figure S6 for a close-up image of filopodia.

Previous work has demonstrated that cofilin induces localized lamellipodia formation and defines the direction of cell movement.^[9a,12] We utilized brief (100 ms), spatially restricted pulses of light to induce localized recruitment of cofilin to F-actin near the leading edge of the cell (Figure 4a

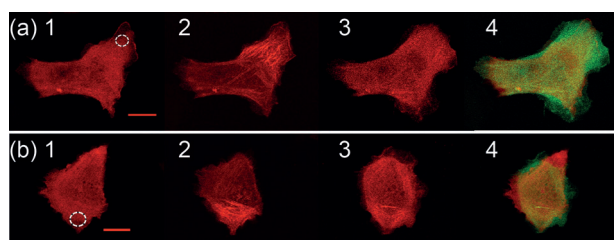


Figure 4. Localized recruitment of cofilin induces protrusive behavior. a) Localized illumination of S3A.S120A-Cof-Cry2-mCh/LifeAct-Cib-GFP-containing MTLn3 cells results in lamellipodia formation in the illuminated region, whereas b) localized illumination in control cells (Cry2-mCh/LifeAct-Cib-GFP) has little effect. 1) Pre-illumination, 2) 10 s (note the recruitment of cofilin to F-actin fibers) and 3) 8 min after illumination. The illumination site is highlighted in (1). 4) Cell protrusion (green) and retraction (red). Significant protrusive activity is observed in (a)(1) at the illumination site, whereas very little change is observed in (b)(4). Scale bar = 10 μm .

and Figure S7). In response to local recruitment of cofilin, cells display rapid lamellipodia formation and an increase in lamellipodia/lamella area (within 30 seconds of stimulus). In contrast, MTLn3 cells containing control constructs (Cry2-mCh) exhibit random walking behavior, little or no lamellipodia formation, and a slight decrease in lamellipodia/lamella area encompassing the site of illumination (Figure 4b and Figure S7). Finally, we employed multiple light pulses to repeatedly recruit cofilin to F-actin and thereby stimulate cell movement over longer distances (Movie S2).

The cofilin knock-out in mice is embryonic lethal,^[15] and a cofilin knock-down in mammalian cell culture impairs cellular behavior.^[16] Consequently, our observation that a genetically expressed photoresponsive cofilin produces discernable cellular effects, even in the presence of endogenous wild-type cofilin, provides the means to perturb cofilin activity without compromising viability. Nonetheless, we also examined the cellular consequences of cofilin photoactivation against a reduced wild-type cofilin activity background. This was achieved by transfecting CofS3A.S120A-Cry2-mCh-expressing MTLn3 cells with LIM-kinase 1 (LIM-K1), which phosphorylates endogenous cofilin at Ser-3 and thus inactivates the ability of cofilin to bind to and remodel the F-actin cytoskeleton.^[9] We note that only endogenous cofilin can be phosphorylated in this fashion, as CofS3A.S120A contains a nonphosphorylatable alanine at the S3A position. LIM-K1 expression resulted in a 50 % increase in endogenous *p*-cofilin levels up to approximately 75 % of total cofilin content (Figure S8). CofS3A.S120A-containing MTLn3 cells, whether or not transfected with LIM-K1, display approximately the same amount of light-induced cell spreading (Figure S5c). This implies that the light-responsive CofS3A.S120A construct serves as the dominant remodeler of the actin cytoskeleton under the illumination conditions described in this study.

In summary, we have developed a genetically expressed photoresponsive F-actin remodelling system that exhibits light-directed motility. Although the design and engineering of genetically expressed photoresponsive proteins has proven challenging, we have found that simply reducing the activity

of native cofilin is all the engineering required to create a background-inactive, light-activatable construct. We note that a significant cellular response is observed even in the presence of endogenous cofilin. This is fortuitous, as it potentially affords the opportunity to create healthy genetically engineered animals in which cofilin action can be subsequently manipulated. For example, recent studies have shown that the invasive and metastatic behavior in breast cancer is driven by the activity of the cofilin pathway.^[17] It should now be possible to directly assess the biological consequences of the abrupt hyperactivation of cofilin as a function of timing and location in animal models.

Received: April 10, 2014

Revised: July 25, 2014

Published online: August 25, 2014

Keywords: cell motility · cofilin · F-actin · optogenetics · protein design

- [1] a) B. N. Goguen, B. Imperiali, *ACS Chem. Biol.* **2011**, *6*, 1164–1174; b) M. J. Kennedy, R. M. Hughes, L. A. Peteya, J. W. Schwartz, M. D. Ehlers, C. L. Tucker, *Nat. Methods* **2010**, *7*, 973–975; c) A. Levskaya, O. D. Weiner, W. A. Lim, C. A. Voigt, *Nature* **2009**, *461*, 997–1001.
- [2] a) B. N. Goguen, B. D. Hoffman, J. R. Sellers, M. A. Schwartz, B. Imperiali, *Angew. Chem. Int. Ed.* **2011**, *50*, 5667–5670; *Angew. Chem.* **2011**, *123*, 5785–5788; b) S. Schröder-Lang, M. Schwarzel, R. Seifert, T. Strunker, S. Kateriya, J. Looser, M. Watanabe, U. B. Kaupp, P. Hegemann, G. Nagel, *Nat. Methods* **2007**, *4*, 39–42; c) M. Stierl, P. Stumpf, D. Udvari, R. Gueta, R. Hagedorn, A. Losi, W. Gartner, L. Peterreit, M. Efetova, M. Schwarzel, T. G. Oertner, G. Nagel, P. Hegemann, *J. Biol. Chem.* **2011**, *286*, 1181–1188; d) Y. I. Wu, D. Frey, O. I. Lungu, A. Jaehrig, I. Schlichting, B. Kuhlman, K. M. Hahn, *Nature* **2009**, *461*, 104–108.
- [3] T. Yin, Y. I. Wu, *Pfluegers Arch.* **2013**, *465*, 397–408.
- [4] D. Chen, E. S. Gibson, M. J. Kennedy, *J. Cell Biol.* **2013**, *201*, 631–640.
- [5] a) S. S. Shekhawat, I. Ghosh, *Curr. Opin. Chem. Biol.* **2011**, *15*, 789–797; b) K. Camacho-Soto, J. Castillo-Montoya, B. Tye, I. Ghosh, *J. Am. Chem. Soc.* **2014**, *136*, 3995–4002.
- [6] a) A. Gautier, A. Deiters, J. W. Chin, *J. Am. Chem. Soc.* **2011**, *133*, 2124–2127; b) C. W. Riggsbee, A. Deiters, *Trends Biotechnol.* **2010**, *28*, 468–475.
- [7] L. Michaelis, M. M. Menten, *FEBS Lett.* **2013**, *587*, 2712–2720.
- [8] K. Moriyama, I. Yahara, *Biochem. J.* **2002**, *365*, 147–155.
- [9] a) M. Ghosh, X. Song, G. Mouneimne, M. Sidani, D. S. Lawrence, J. S. Condeelis, *Science* **2004**, *304*, 743–746; b) K. Moriyama, K. Iida, I. Yahara, *Genes Cells* **1996**, *1*, 73–86; c) B. J. Pope, S. M. Gonsior, S. Yeoh, A. McGough, A. G. Weeds, *J. Mol. Biol.* **2000**, *298*, 649–661.
- [10] a) M. Sidani, D. Wessels, G. Mouneimne, M. Ghosh, S. Goswami, C. Sarmiento, W. Wang, S. Kuhl, M. El-Sibai, J. M. Backer, R. Eddy, D. Soll, J. Condeelis, *J. Cell Biol.* **2007**, *179*, 777–791; b) L. K. Doolittle, M. K. Rosen, S. B. Padrick, *Methods Mol. Biol.* **2013**, *1046*, 273–293.
- [11] J. Riedl, A. H. Crevenna, K. Kessenbrock, J. H. Yu, D. Neukirchen, M. Bista, F. Bradke, D. Jenne, T. A. Holak, Z. Werb, M. Sixt, R. Wedlich-Soldner, *Nat. Methods* **2008**, *5*, 605–607.
- [12] E. A. Vitriol, A. L. Wise, M. E. Berginski, J. R. Bamburg, J. Q. Zheng, *Mol. Biol. Cell* **2013**, *24*, 2238–2247.
- [13] X. Song, X. Chen, H. Yamaguchi, G. Mouneimne, J. S. Condeelis, R. J. Eddy, *J. Cell Sci.* **2006**, *119*, 2871–2881.
- [14] R. B. Lichtner, M. Wiedemuth, C. Noeske-Jungblut, V. Schirmacher, *Clin. Exp. Metastasis* **1993**, *11*, 113–125.
- [15] C. B. Gurniak, E. Perlas, W. Witke, *Development Dev. Biol.* **2005**, *278*, 231–241.
- [16] J. von Blume, J. M. Duran, E. Forlanelli, A. M. Alleaume, M. Egorov, R. Polishchuk, H. Molina, V. Malhotra, *J. Cell Biol.* **2009**, *187*, 1055–1069.
- [17] W. Wang, R. Eddy, J. Condeelis, *Nat. Rev. Cancer* **2007**, *7*, 429–440.